ELSEVIER

Polymer 40 (1999) 5655–5664

polymer

Comparison of gas transport and sorption in the ladder polymer BBL and some semi-ladder polymers

Catherine M. Zimmerman[1], William J. Koros*

Department of Chemical Engineering, The University of Texas at Austin, Austin, TX 78712-1062, USA

Received 18 September 1998; received in revised form 19 October 1998; accepted 27 October 1998

Abstract

Gas separation membrane permselectivity is often improved by the introduction of stiffer polymeric backbone structures. This chain rigidity enables the polymeric segments to discriminate more selectively between penetrants of different size. Although not extensively reported in the literature, ladder and semi-ladder polymers formed from tetraamines and dianhydrides potentially provide rigid polymeric structures void of significant rotational mobility. This work examines the gas transport and sorption properties of BBL, a ladder polymer synthesized from 1,2,4,5-tetraaminobenzene tetrahydrochloride and 1,4,5,8-naphthalenetetracarboxylic acid. In addition, the behavior of He, CO_2, O_2, N_2, and CH_4 permeability, diffusion, and sorption coefficients with temperature is examined and shown to follow the Arrhenius and van't Hoff relationships. The near-ambient permeation properties of BBL are also compared with other previously reported semi-ladder polymers formed using polypyrrolone chemistry. These semi-ladder polymers incorporate both flat, packable monomers such as those used to form BBL as well as bulky monomers to inhibit chain packing.

Keywords: BBL; Membrane separation processes; Gas transport

1. Introduction

Polymer gas transport structure–property relationships have been studied extensively over the past two decades [1,2]. In flexible polymers, molecular scale gaps in the polymer matrix are formed by short time scale chain motions [2]. Gas diffusion in such materials occurs by a transient gap of sufficient size being created such that the penetrant is able to execute a diffusive jump. In general, desirable gas transport property improvements have been achieved by tailoring polymeric structures using two principles [1]. Bulky groups in the polymer backbone inhibit intersegmental packing and often increase the permeability. Polymeric segments that reduce mobile linkages in the polymer backbone tend to increase the polymer permselectivity. While polyimides, a more rigid polymer family than polysulfone or polycarbonate, often exhibit enhanced polymeric permselectivities, additional improvements may be attainable by investigating even more rigid structures such as ladder and semi-ladder polymers. As a consequence of eliminating mobile linkages in the backbone, the ''picture'' of gas diffusion in an extremely rigid polymer differs from that of flexible polymers and will be discussed in this work.

Since the early 1960s, ladder polymers have been investigated because of their high thermal stability and potential electrical conductivity [3]. Despite this, only a limited number of studies have investigated the potentially attractive gas transport properties of ladder or semi-ladder polymers [4–11]. Depending on the heterocycle (five or six member rings) formed in the process, the polymers are given different descriptive names. In several previous studies, the electrical conductivity of BBL, an extremely rigid benzimidazobenzophenanthroline-type polymer, has been investigated following heavy doping [12–15]. Yet, no prior studies have characterized gas transport in this material even though the rigid, ladder structure makes it potentially attractive. This work characterizes gas permeation, diffusion, and sorption in BBL and compares it to other semi-ladder polymers with some structural similarities.

2. Theory and background

The permeability coefficient, P_i, of a penetrant i is commonly used to measure the ease of gas transport through

* Corresponding author. Tel.: + 1-512-471-5238; fax: + 1-512-471-7060.

[1] Current Address: Amoco Chemicals, 150 W. Warrenville Rd. C-8, Naperville, IL 60563, USA.

0032-3861/99/$ - see front matter
PII: S0032-3861(98)00777-0

a material and is defined as

$$P_i = \frac{N_i}{\Delta p_i/\ell}, \tag{1}$$

where Δp_i is the partial pressure driving force across the membrane and ℓ the membrane thickness. The permeability coefficient, P_i, is the product of a kinetic parameter, D_i, the average diffusion coefficient and a thermodynamic parameter, S_i, the sorption coefficient.

$$P_i = D_i \cdot S_i. \tag{2}$$

The sorption coefficient is measured as the secant slope of the sorption isotherm at the upstream pressure when the membrane downstream pressure is negligible. The sorption coefficient is affected by penetrant condensibility, polymer–penetrant interactions, and free volume in glassy polymer matrices. Upon experimentally measuring the permeability and sorption coefficients, the effective average diffusion coefficient can be calculated by dividing the former by the latter. In traditional polymers, the diffusion coefficient is proportional to the frequency at which gaps of sufficient volume are opened next to the penetrant, allowing it to make a diffusive jump. Factors such as penetrant size, chain packing, polymer chain segment mobility, and cohesive energy of the polymer govern the rate of diffusion [16]. In rigid materials such as carbon molecular sieves (CMS) and zeolites, penetrant diffusion occurs when the molecule is able to overcome the repulsive forces associated with passing through the well-defined constricted regions [17]. For these rigid materials, the penetrant and constricted region dimensions primarily affect the rate of diffusion.

In gas separations, membrane permselectivity is characterized by a separation factor, $\alpha_{A/B}$, which is a function of the mole fractions of the two components. A and B, in the upstream and downstream, x_i and y_i, respectively.

$$\alpha_{A/B} = \frac{(y_A/y_B)}{(x_A/x_B)}. \tag{3}$$

When the downstream pressure is negligible compared to the upstream, Eq. (3) is approximated by an ''ideal'' separation factor, $\alpha^*_{A/B}$, which equals the ratio of the permeabilities of the two gases. The permselectivity equals the product of the diffusivity selectivity and sorption selectivity.

$$\alpha^*_{A/B} = \frac{P_A}{P_B} = \left(\frac{D_A}{D_B}\right)\left(\frac{S_A}{S_B}\right). \tag{4}$$

In previously reported polymeric materials, improvements in the permselectivity have generally been accomplished by increases in the diffusivity selectivity. The diffusivity selectivity term in Eq. (4) relates to the ability of the polymer matrix to selectively separate penetrants based on molecular size. As a result, it is governed by the chain backbone rigidity and intersegmental packing [18]. For gas mixtures, the sorption selectivity depends primarily on the condensibility of the two penetrants. Studies have demonstrated that this factor is difficult to increase without simultaneous decreases in diffusivity selectivity because of plasticization induced by interactions between the matrix and penetrant [19].

Equilibrium gas sorption concentration in glassy polymers is generally described by the dual mode model which states that the overall concentration is a sum of populations in the Henry's Law and Langmuir molecular environments [20–22].

$$C = C_D + C_H. \tag{5}$$

The Henry's Law concentration, C_D, accounts for the penetrants in a dissolved state similar to the sorption environment in rubbery polymers. The Langmuir concentration, C_H, describes the molecules sorbed into microvoids that are characteristic of non-equilibrium glassy polymers. These microvoids form as the polymer is cooled below its glass transition temperature, which inhibits polymer chain relaxation.

The pressure dependence of the equilibrium gas concentration can be described by Henry's Law and the Langmuir isotherm for C_D and C_H, respectively.

$$C = k_D p + \frac{C'_H b p}{1 + bp}, \tag{6}$$

where k_D is the Henry's Law coefficient, b the Langmuir affinity constant, and C'_H the Langmuir capacity constant. The sorption coefficient of penetrant A, S_A, is the secant slope of the sorption isotherm and given by

$$S_A = \frac{C}{p} = k_D + \frac{C'_H b}{1 + bp}. \tag{7}$$

The temperature dependent gas permeability, diffusion, and sorption coefficients of a polymer, lacking thermal transitions in the given temperature range, are described by the two Arrhenius relationships and a van't Hoff relationship, respectively [16].

$$P = P_0 \exp\left[\frac{-E_p}{RT}\right], \tag{8}$$

$$D = D_0 \exp\left[\frac{-E_d}{RT}\right], \tag{9}$$

$$S = S_0 \exp\left[\frac{-H_s}{RT}\right], \tag{10}$$

where P_0, S_0, and D_0 are pre-exponential factors, E_p the activation energy for permeation, E_d the activation energy for diffusion, H_s the heat of sorption, R the universal gas constant, and T the absolute temperature.

Insight into the effects of temperature on permeability can be attained by examining its effect on the sorption and diffusivity coefficients. Generally, the permeability coefficient increases with temperature with lower permeable membranes being more sensitive to temperature changes. As diffusion in polymers is an activated process, when the temperature is increased, the diffusion coefficient increases yielding a positive activation energy for diffusion. The

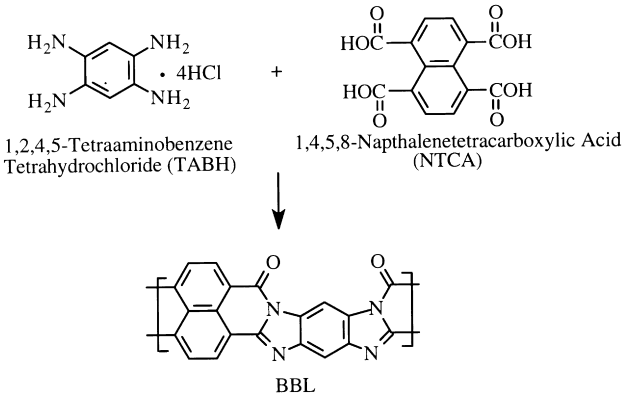

Fig. 1. Solution polymerization synthesis of BBL.

activation energy for diffusion essentially describes the energy required for a penetrant to make a diffusive jump from one equilibrium site to another. The magnitude of this energy is a function of the polymer chain packing (or cohesive energy density), polymeric chain rigidity, and the penetrant size. In most cases, gas solubility decreases with increasing temperature resulting in a negative heat of sorption. Combination of Eqs. (8)–(10) indicates that the activation energy of permeation is simply the sum of the activation energy of diffusion and heat of sorption.

$$E_p = E_d + H_s \tag{11}$$

Recent work by Singh and Koros compared and analyzed the O_2/N_2 diffusivity selectivities of three gas separation materials: zeolite 4A, CMS, and an upper bound polypyrrolone [17] and concluded that the superior gas transport properties of the molecular sieves relative to the polymer can be attributed to high ''entropic selectivities''. As previously shown, the diffusivity selectivity can be described as approximately the product of enthalpic and entropic terms [17]

$$\frac{D_A}{D_B} = \underbrace{\exp\left[\frac{-\Delta E_{A,B}}{RT}\right]}_{\textit{Energetic Selectivity}} \quad \underbrace{\exp\left[\frac{\Delta S_{A,B}}{R}\right]}_{\textit{Entropic Selectivity}} \tag{12}$$

where $\Delta E_{A,B}$ is the difference in the activation energy of diffusion for penetrants A and B while $\Delta S_{A,B}$ is the difference in activation entropy of diffusion. The comparison of experimental measurements and theoretical calculations show that the exceptional O_2/N_2 diffusivity selectivities of zeolite 4A and CMS arise because of the difference in the rotational degrees of freedom of O_2 and N_2 in the molecular sieving media, which primarily affects the entropic selectivity term.

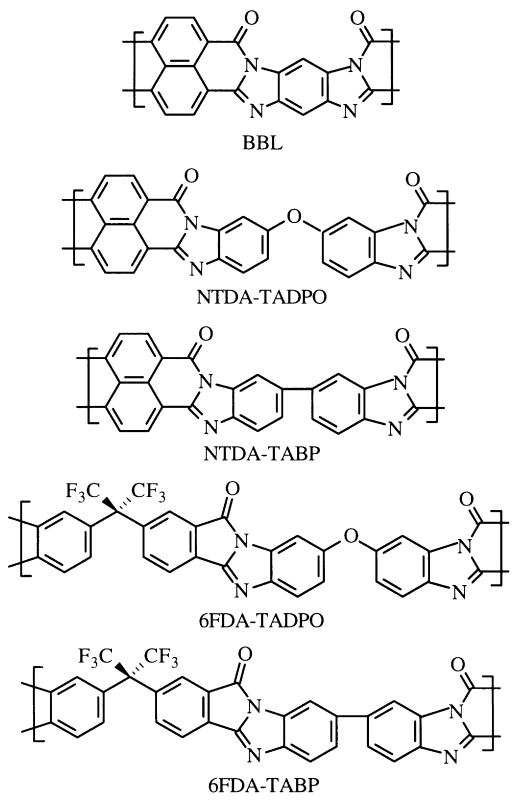

Fig. 2. Polymeric structures used in structure–property comparison.

3. Experimental

3.1. Materials

BBL was prepared by the method previously described in the literature [23,24], which is the polycondensation reaction of 1,2,4,5-tetraaminobenzene tetrahydrochloride (TABH) with 1,4,5,8-napthhalenetracarboxyclic acid (NTCA) shown in Fig. 1. As a result of the high degree of conjugation, the polymer was only soluble in strong protonic acids such as methanesulfonic, which complicated the casting process because of the high boiling point and corrosivity associated with acids. The appropriate amount of polymer was dissolved in methanesulfonic acid (99%) to form a 1.0 wt.% solution. The solution was placed in a leveled glass petri dish positioned on a hot plate. The petri dishes were covered with a glass funnel possessing a Teflon® filter dust cover on the top of the funnel. The glass funnel controlled the rate of solvent evaporation and prevented dust from falling on the film. The bottom surface of the petri dish was maintained at 140°C until a polymer film pulled away from the dish. The resulting film and film fragments were dried under vacuum at 150°C for 3 d. The film was then submerged in methanol to extract any residual acid for 10 h. After repeating the extraction procedure again twice, the films were dried under vacuum at 150°C for 1 d.

Dense BBL films were also received from Dr. Fred Arnold at Wright Patterson Air Force Base. Used in permeation experiments, these films consisted of higher molecular weight BBL which reduced the tendency of film tearing. These films were prepared in a similar manner to that

Table 1
Kinetic diameters [27] and critical temperatures [28] of penetrants

Penetrant	Kinetic diameter (Å)	Critical temperature (K)
He	2.6	5
CO_2	3.3	304
O_2	3.46	154
N_2	3.64	126
CH_4	3.8	191

described earlier except that they were cast in a sublimator under vacuum.

This work compares the BBL gas transport and sorption properties to those of some semi-ladder polymers such as NTDA–TADPO, NTDA–TABP, 6FDA–TADPO, and 6FDA–TABP as shown in Fig. 2. The results to be presented show how changes in flexible linkages and substituent size affect the gas transport properties. Using the same dianhydride as BBL but a different tetraamine, Zhou and Lu [5] studied gas transport in NTDA–TADPO and NTDA–TABP. Unlike BBL, the NTDA–TADPO possesses a flexible ether linkage about which molecular rotation occurs in the 3,3′,4,4′-tetraamino-diphenyl-oxide (TADPO) segments. Similarly, the NTDA–TABP possesses tetraaminobiphenyl (TABP) segments, which again have flexible linkages within the aromatic polymer. Koros and Walker investigated 6FDA–TADPO and 6FDA–TABP gas transport [7,25]. Although these structures possess the tetraamine segments identical to the NTDA-based polymers, they incorporate the bulky 6FDA group in the polymer chain to inhibit packing and promote diffusion through the polymer matrix. In addition, temperature dependence of the BBL and 6FDA–TADPO gas transport properties have been compared to provide additional insights into the factors influencing gas transport in these very different materials [26].

3.2. Permeation and sorption

Using the manometric, or constant volume, method, permeation properties of He, CO_2, O_2, N_2 and CH_4 were measured. Ultra-high purity gases (99.99%) supplied by Praxair were used for all experiments. The kinetic diameters from the Lennard–Jones interaction potential [27] and critical temperatures [28] of the penetrants studied are reported in the Table 1. The laboratory equipment used in these experiments has previously been described in detail [29,30]. Measurements were completed using a high pressure upstream and vacuum downstream. Permeability measurements were made at pressures up to 10 atm (except for O_2) and at temperatures of 35°C, 50°C, 65°C, and 80°C.

Polymeric gas sorption measurements of He, CO_2, O_2, N_2, and CH_4 were performed using a high-temperature dual-volume sorption apparatus. A previous report has described the laboratory apparatus [30]. The dual-volume apparatus consists of a cell and reservoir volume while the flat sheet polymeric films were placed in the cell. Sorption isotherms were measured using interval experiments which successively increased the penetrant pressure or concentration. Sorption measurements were performed at temperatures of 35°C, 50°C, 65°C, and 80°C.

Table 2
Polymeric physical properties

Polymer	T_g (°C)	*d*-spacing (Å)	Density (g/cm^3)	FFV
BBL	not observed	3.4, 7.6	1.481	0.109
NTDA–TADPO[a]	—	3.5	—	—
NTDA–TABP[a]	—	3.4	—	—
6FDA–TADPO[b]	375	5.9	1.405	0.196
6FDA–TABP[b]	370	5.7	1.399	0.189

[a] Data from [5].
[b] Data from [6].

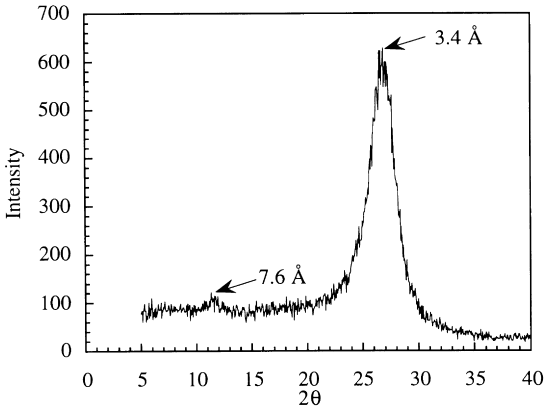

Fig. 3. Wide angle X-ray diffraction spectra of BBL.

3.3. Physical properties

The flat BBL chemical structure suggests that the polymer chains will pack efficiently. As shown in Table 2, the BBL glass transition temperature (T_g), density, fractional free volume (FFV), and *d*-spacing from x-ray diffraction experimentally confirm this hypothesis. The potential BBL glass transition temperature was investigated with differential scanning calorimetry (DSC) using a Perkin Elmer DSC 7. BBL fails to exhibit a glass transition temperature prior to degradation, which is not surprising because of the immense polymeric chain rigidity. Unlike BBL, 6FDA–TADPO and 6FDA–TABP exhibit glass transition temperatures indicating their structures have greater mobility, which is consistent with the chemical structures.

Wide angle x-ray diffraction is an analytical method that provides information about the polymeric intersegmental packing, which is described by the average *d*-spacing. A Philips PW 1710 diffractometer was used for the film sample measurements with Cu Kα radiation of 1.54 Å wavelength. The BBL x-ray diffraction spectra, shown in Fig. 3, exhibits average *d*-spacings at 3.4 and 7.6 Å, which agree with previous reports [31,32]. Again indicating an

Table 3
Permeability coefficients and permselectivities of BBL and other semi-ladder polymers at 35°C and 10 atm (O_2 at 3 atm)[a]

Polymer	P_{He}	P_{O_2}	P_{CO_2}	P_{He}/P_{CH_4}	P_{O_2}/P_{N_2}	P_{CO_2}/P_{CH_4}
BBL	0.54	0.021	0.12	320	8.1	71
NTDA–TADPO[b]	—	0.314	—	—	7.7	—
NTDA–TABP[b]	—	0.862	—	—	7.1	—
6FDA–TADPO[c]	90.2	7.9	27.4	172	6.5	52.2
6FDA–TABP[c]	138	16.4	63.6	100	5.5	46.2

[a] 1 Barrer $= 10^{-10}$(cm^3 (STP) cm)/(cm^2 s cm Hg).
[b] Data from [5] Permeation measurements at 1 atm and 30°C.
[c] Data from [6].

extremely tightly packed matrix, the 3.4 Å *d*-spacing has been shown to correspond to the face-to-face interchain packing while the 7.6 Å *d*-spacing relates to the side-to-side packing [31]. Compared to other amorphous, glassy polymers that generally exhibit broad peaks, the 3.4 Å peak is relatively sharp suggesting greater chain packing order in BBL.

The specific degree of chain packing is difficult to accurately *quantify* with x-ray diffraction because of the lack of long range order in polymers. Rather, the technique only provides a method for qualitative comparison such as with the NTDA and 6FDA-based polymers. Similar to BBL, NTDA–TADPO and NTDA–TABP possess the flat, packable naphthalene-based dianhydride. As a result, these materials exhibit rather small *d*-spacings ranging from 3.4–3.5 Å. Flexible linkages in both polymers do not significantly alter the *d*-spacing when compared to BBL. In sharp contrast, 6FDA incorporation in 6FDA–TADPO and 6FDA–TABP produces *d*-spacings over 2 Å larger, 5.7–5.9 Å, than the NTDA-based polymers.

The FFV is a quantity that indicates the relative degree of packing between the polymer chain segments. The FFV is the ratio of the specific free volume to the specific volume as estimated by the method of Lee [33]. The specific free volume calculation, which uses the group contribution method of Van Krevelen [34], is determined by the difference between the experimentally measured specific volume and the specific occupied Van der Waals volume given by Bondi [35].

FFV calculations complement the tightly packed polymeric matrix physical picture given by x-ray diffraction. The BBL FFV, 0.109, is *extremely* low compared to other more traditional gas separation materials such as polycarbonate and polysulfone possessing FFVs of 0.164 and 0.156, respectively [36,37]. Again, based on the chemical structure, the low BBL FFV is anticipated. The 6FDA-based polymer FFVs are 73%–80% greater than BBL, which are undoubtedly caused by the bulky, packing inhibiting fluorine atoms in the 6FDA.

Although commonly used, an aqueous gradient column is not suitable for the density measurement of BBL because of the large amount of water this polymer type has been reported to sorb [38]. As the polymer macroscopic density at 25°C falls between that of carbon tetrachloride and chloroform, the density was experimentally measured from a series of solvent mixtures. Independent pure solvent sorption experiments confirmed that negligible carbon tetrachloride and chloroform were sorbed over the time span of the density experiments. To a beaker of chloroform, carbon tetrachloride was added incrementally and mixed until the polymer film piece started to sink. Similarly, to a beaker of carbon tetrachloride, chloroform was added incrementally and mixed until the polymer film started to float off the bottom of the beaker. Extreme caution was given to keep the beaker tightly covered during the experiment to avoid any solvent evaporation. The solution density was closely approximated from the volume of each solvent known to be in the mixture. Although the calculated densities from the two experiments were very similar (± 0.002 g/cm^3), the values were averaged. Although density measurements directly measure a polymer physical property, they are difficult to relate to the degree of interchain packing. Density measurement values can be distorted by heavy elements such as fluorine, relative to carbon, hydrogen, and nitrogen, whereby hindering a comparison of the intersegmental packing using only this physical property. For the polymers compared in this work, the FFV serves as better measurement of the relative degree of chain packing in the polymer matrix compared to density measurements.

4. Results and discussion

4.1. Gas transport and sorption

Table 3 compares the gas permeabilities and permselectivities of BBL, NTDA–TADPO, NTDA–TABP, 6FDA–TADPO, and 6FDA–TABP. For these materials, the dianhydride structure predominantly controls the relative permeability. For example, 6FDA–TADPO and 6FDA–TABP exhibit O_2 permeabilities 9–780 times greater than the NTDA-based polymers. This observation, undoubtedly, results from the significantly higher FFV in the 6FDA-based polymers compared to the NTDA-based polymers. Tetraamine structural changes more subtly affect the O_2 permeability. Replacement of TAB in BBL with TADPO results in a permeability increase of over an order of magnitude, which likely results from the ether linkage with rotational mobility in TADPO. A tetraamine change from TADPO to TABP in both the NTDA and 6FDA-based polypyrrolones yields an O_2 permeability increase of over 100% despite a FFV decrease and removal of a flexible bond. Similar effects occur with He and CO_2 permeation. Although this result is anomalous, a difference in FFV *distribution* throughout the polymer matrix [6] may describe the observation. In previous studies, both the FFV and its distribution have been suggested to influence gas transport [39]; however,

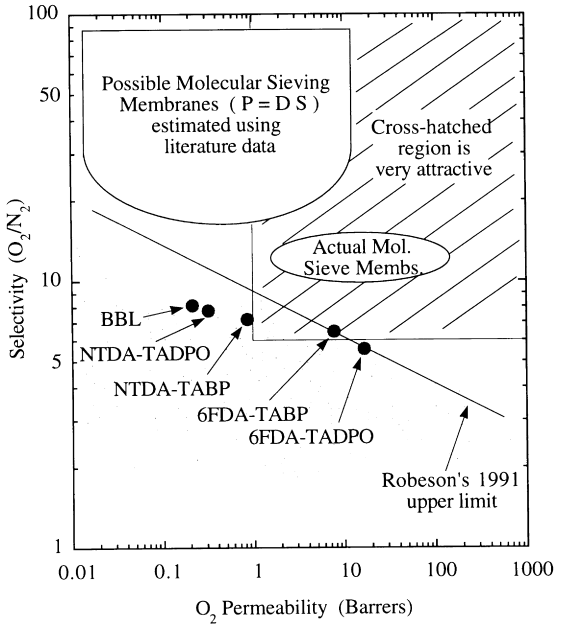

Fig. 4. BBL and semi-ladder polymer performances compared to O_2/N_2 trade-off limit.

no independent corroboration of this hypothesis has been achieved.

Commonly observed in polymeric materials, the O_2/N_2 permselectivity decreases with increasing O_2 permeability in this group of polymers. The He/CH_4 and CO_2/CH_4 selectivities also display a similar trend with permeability. BBL exhibits the highest O_2/N_2 permselectivity, 8.1, coupled with the lowest O_2 permeability, 0.021 Barrers. Upon addition of 6FDA, the permselectivity decreases indicating a lower ability to discriminate between the similarly sized O_2 and N_2 molecules, which most likely arises from the higher free volume 6FDA polymer matrices.

Polymeric membrane materials typically exhibit a so-called performance trade-off between O_2 permeability and O_2/N_2 selectivity [40]. When comparing BBL and the semi-ladder polymers to other polymeric gas separation materials in Fig. 4, the transport properties are seen to fall below or on the upper limit of performance. The combination of a rigid structure and tight chain packing leads to an extremely low BBL O_2 permeability (0.021 Barrers). Unlike flexible yet packable polymers, diffusion in such rigid materials is not thought to occur by segmental motions occurring throughout the polymer matrix. Since x-ray diffraction indicates

Table 4
Diffusion coefficients and diffusivity selectivities of BBL at 35°C and 10 atm (O_2 at 3 atm)[a]

Polymer	D_{He}	D_{O_2}	D_{CO_2}	D_{He}/D_{CH_4}	D_{O_2}/D_{N_2}	D_{CO_2}/D_{CH_4}
BBL	380	3.1	3.8	1600	6.6	16

[a] 10^{-10} cm^2/s.

Table 5
Sorption coefficients and sorption selectivities of BBL at 35°C and 10 atm (O_2 at 3 atm)[a]

Polymer	S_{He}	S_{O_2}	S_{CO_2}	S_{He}/S_{CH_4}	S_{O_2}/S_{N_2}	S_{CO_2}/S_{CH_4}
BBL	0.11	0.52	2.4	0.20	1.2	4.5

[a] $((cm^3(STP))/(cm^3(polymer)\ atm)$.

extremely small average center-to-center chain distances, diffusion in the BBL matrix most likely occurs through small regions of imperfect packing. Considering the rigid structure of BBL, the O_2/N_2 permselectivity is somewhat disappointing when compared to other polymers. The result of this work is, therefore, extremely important in indicating that simply increased chain rigidity has diminishing returns when unaccompanied by chain disruptions to promote gas diffusion. It likely that the permselectivity is not as high as expected because diffusion generally occurs through regions of disrupted packing with less diffusive selectivity than expected. Based on this structure–property study, it is possible that a material possessing bulky groups to promote diffusion combined with no flexible linkages may potentially exhibit even more favorable gas transport properties than those observed here. Processing would, of course, be a major challenge for such a material.

As discussed in an earlier section, the permeability can be partitioned into a diffusion and a sorption coefficient, which are principally kinetic and thermodynamic in nature, respectively. Table 4 reports the diffusion coefficients and diffusivity selectivities of He, CO_2, O_2, N_2, and CH_4 in BBL. Similarly, Table 5 lists the sorption coefficients and sorption selectivities determined by the dual-volume method described previously. Using permeation and diffusion coefficients from dynamic methods, Zhou and Lu calculated O_2/N_2 sorption coefficients and selectivities for the NTDA-based polymers [1,12]. The O_2/N_2 sorption selectivities reported were *less than one* where numerous other polymeric membrane materials studied by various researchers range between 1.1 and 2.0 [2]. For essentially all polymeric

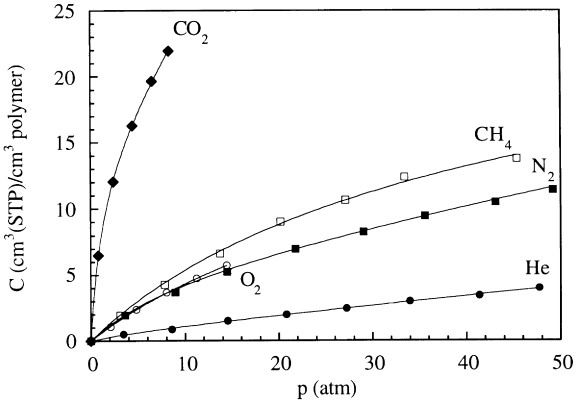

Fig. 5. BBL sorption isotherms at 35°C.

Table 6
Dual mode parameters of CO_2, CH_4 and N_2 for BBL at 35°C

Gas	k_D((cm^3(STP))/(cm^3 atm))	C'_H((cm^3(STP))/cm^3)	b(atm^{-1})
CO_2	1.13	14.6	0.745
CH_4	0.115	13.0	0.048
N_2	0.113	7.88	0.059

materials, penetrant condensibility governs sorption coefficients. Hence, O_2 sorbs more in polymeric materials, because it possesses a higher critical temperature than N_2 [28]. As a result, the NTDA-based polymer sorption data was not used to form a sorption and diffusion coefficient structure–property comparison with BBL, because polymeric O_2/N_2 sorption selectivities less than one are highly unlikely.

After comparing the diffusion and sorption components of the BBL permeability, it is evident that the diffusion coefficient primarily controls the permeability and permselectivity. For example, BBL exhibits an O_2/N_2 permselectivity of 8.1 while the diffusivity and sorption selectivities are 6.6 and 1.2, respectively.

BBL sorption isotherms at 35°C are shown in Fig. 5. Measurements for He, N_2, and CH_4 were completed up to approximately 50 atm while O_2 measurements only reached about 15 atm because of safety reasons. Measurements of CO_2 sorption, limited to 10 atm, avoided any possible plasticization and conditioning effects, which would lead to erroneous sorption measurements at higher temperatures. The isotherm shapes, which curve toward the pressure axis, indicate sorption can be described by the dual-mode model given by Eq. (7). At lower pressures, penetrants sorb in both the Henry's law and Langmuir environments of the polymer. The Henry's law environment accounts for penetrants in a dissolved mode while the Langmuir environment describes penetrants sorbed in the excess or unrelaxed volume present in glassy polymers.

The dual mode parameters, which characterize sorption in BBL and other polymeric materials, were determined by a least squares treatment and are shown in Table 6 for CO_2, CH_4, and N_2. The C'_H term is the hole saturation constant, which measures the sorption capacity of the unrelaxed volume. As it is influenced by the gas condensibility, C'_H decreases with the sorption coefficient where $N_2 < CH_4 < CO_2$ as shown in Tables 5 and 6. The hole affinity constant, b, represents the rate constant ratio of penetrant sorption to desorption in holes or defects. Therefore, the parameter characterizes the penetrant's tendency to sorb in the Langmuir environment. Similarly, the Henry's law coefficient, k_D, characterizes the affinity of the penetrant to sorb in the dissolved environment. A substantial difference in Langmuir site affinity for CO_2 compared to CH_4 and N_2 is present since the hole affinity constants for CH_4 and N_2 are similar. A similar, although less pronounced, trend in the hold affinity constant is observed for polycarbonate. For polycarbonate, the hole affinity constant is 0.262 atm^{-1} for CO_2 and decreases to 0.084 and 0.056 atm^{-1} for CH_4 and N_2, respectively [22]. In general, this observation is expected considering that CO_2 is significantly more condensible than CH_4 and N_2.

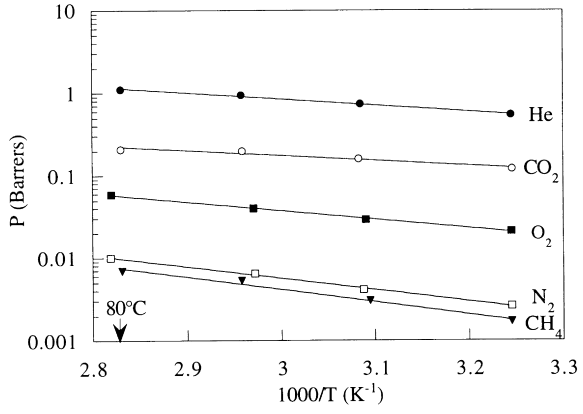

Fig. 6. Temperature dependence of BBL permeabilities at 10 atm (O_2 at 3 atm).

4.2. Temperature dependence of gas transport and sorption

The temperature dependence of the He, CO_2, O_2, N_2, and CH_4 permeabilities was measured at 35°C, 50°C, 65°C, and 80°C. Upstream pressures of 10 atm for He, CO_2, N_2, and CH_4 were used while O_2 pressures never exceeded 3 atm. Fig. 6 illustrates the permeability temperature dependence over the aforementioned temperature range, which does not encompass any polymeric thermal transitions. In Fig. 6, the permeability data plotted as a function of inverse temperature exhibit an Arrhenius type behavior. The steeper N_2 and CH_4 Arrhenius plot slopes indicate that temperature more strongly affects permeation of these gases than the smaller He, O_2, and N_2 molecules.

Similarly, temperature dependent sorption coefficients were measured using the dual volume sorption apparatus described earlier. Again, CO_2, O_2, N_2, and CH_4 were studied at temperatures between 35°C and 80°C. The temperature dependence of the He sorption coefficient is not presented because of extremely low gas sorption at elevated temperatures, which hinders accurate measurements. BBL sorption coefficients as a function of inverse temperature are shown in Fig. 7 to exhibit van't Hoff behavior.

The BBL activation energies and heats of sorption of He, CO_2, O_2, N_2, and CH_4 are tabulated in Table 7. In addition, the respective pre-exponential factors are reported in Table 8. The method for calculating the uncertainties associated with the activation energies, heats of sorption, and pre-exponential factors have been previously reported [41,42]. The uncertainties associated with these properties for BBL are included in Tables 7 and 8. Using Arrhenius or van't Hoff relationships, the activation energies for permeation, heats of sorption, and pre-exponential factors were determined. Activation energies for diffusion and the respective

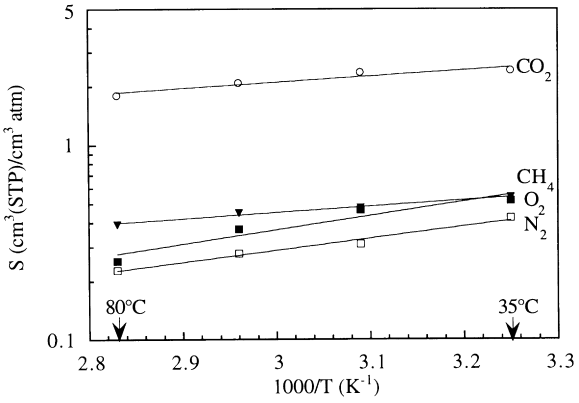

Fig. 7. Temperature dependence of BBL sorption coefficients at 10 atm (O_2 at 3 atm).

pre-exponential factors were calculated using Eqs. (8), (9) and (10). The activation energies and heats of sorption reported are strictly valid only in the temperature region investigated, 35°C–80°C. The activation energies, heats of sorption, and pre-exponential factors enable the determination of permeability, sorption, and diffusion coefficients at any temperature within the range studied.

The activation energy for permeation has contributions from both the activation energy for diffusion and the heat of sorption. For all gases except for CO_2, which exhibits a large sorption coefficient, penetrant size and polymer structure primarily affect the activation energies for permeation and diffusion. As shown in Table 7, the activation energy for permeation increases in the order $CO_2 < He < O_2 < N_2 < CH_4$, which is the identical order of increasing penetrant size shown in Table 1 with the exception of CO_2. In general, this is consistent with previous temperature dependent gas transport studies of these gases in polycarbonates, polyimides, and polypyrrolones [26,42–43].

Penetrant size also strongly affects the activation energy for diffusion. In most cases, the temperature dependence of the diffusion coefficient increases with penetrant size.

Table 7
Activation energies and heats of sorption for BBL and 6FDA – TADPO[a]

Gas	E_p	E_d	H_s
	BBL		
He	3.5 ± 0.2	—	—
CO_2	2.8 ± 0.3	4.2 ± 0.5	−1.4 ± 0.2
O_2	4.8 ± 0.2	8.1 ± 0.6	−3.3 ± 0.4
N_2	6.4 ± 0.3	9.2 ± 0.5	−2.8 ± 0.2
CH_4	6.9 ± 0.4	8.3 ± 0.4	−1.4 ± 0.1
	6FDA–TADPO[b]		
O_2	2.0	5.3	− 3.3
N_2	3.1	6.2	− 3.1

[a] kcal/mol.
[b] Data from [26].

Table 8
Pre-exponential factors for BBL

Gas	P_0 (Barrers)	D_0 (10^{-6} cm²/s)	S_0((10^{-2}cm³(STP))/(cm³ atm))
He	150 ± 39	—	—
CO_2	12 ± 5.7	0.36 ± 0.16	25 ± 7.3
O_2	55 ± 17	170 ± 89	0.25 ± 0.15
N_2	82 ± 38	150 ± 58	0.42 ± 0.11
CH_4	140 ± 76	21 ± 8.8	5.1 ± 0.58

Temperature increases tend to exhibit a greater effect on large penetrant diffusion relative to small ones. For example, O_2 usually exhibits a lower E_d than N_2 since it is smaller. Table 7 reports that the E_d value for CH_4 is less than N_2. Although the Lennard–Jones kinetic diameters in Table 1 indicate that CH_4 is larger than N_2, this may be inadequate characterization of the two penetrants. The Lennard–Jones size parameter is a ''tumbling diameter'', which considers the molecule to be effectively a sphere. This is probably not a bad approximation for CH_4. On the other hand, N_2 is spherocylindrical with a length and width of 4.07 and 3.09 Å, respectively, as determined from the Kihara potential [17]. When considering this more accurate description of the molecular dimensions, it is obvious that the ''major'' N_2 dimension is greater than the CH_4 diameter while the ''minor'' dimension is less. Hence, it seems that analysis of the effects of N_2 and CH_4 size on E_d may need to consider the subtle differences in molecular size and shape of the penetrants in these hyper rigid matrices. One must be cautious not to over-interpret these data, as the difference between these activation energies is actually encompassed by the calculated uncertainties. Additional work is needed to better define the apparent trends noted earlier.

Thermodynamic properties, such as the penetrant critical temperature, significantly affect the heat of sorption. As sorption is exothermic in nature, the most condensible gas studied, CO_2, is expected to exhibit the lowest (most negative) heat of sorption. After comparing the heats of sorption tabulated in Table 7, they increase in the order $O_2 < N_2 < CH_4 = CO_2$, which shows deviations from their relative condensibilities, or critical temperatures shown in Table 1. The CH_4 and CO_2 heat of sorption deviations from the penetrant condensibility trend are potentially explained by considering the two main factors influencing the heat of sorption. A *negative* enthalpy, guided by the penetrant critical temperature, is associated with gaseous sorption in the polymer matrix. In contrast, a *positive* enthalpy is required to create a sorption site [44]. For BBL sorption, it is possible that the heat necessary to create a sorption site for the CH_4 and CO_2 molecules, which are large and highly sorbing, respectively, is significantly greater than in more traditional polymeric materials because of the rigid, tightly packed BBL structure. Hence, the heats of sorption for CH_4 and CO_2 are not as low as anticipated because of the larger positive contribution.

Table 9
Energetic and entropic contributions to O_2/N_2 diffusivity selectivity in BBL and 6FDA–TADPO

Polymer	D_{O_2}/D_{N_2}	$\Delta E_{d,O_2,N_2}$ kcal/mol	Energetic selectivity	Entropic selectivity
BBL	6.6	− 1.1	6.0	1.1
6FDA–TADPO[a]	4.8	− 0.90	4.3	1.1

[a] Data from [42,45].

4.3. BBL and 6FDA–TADPO: comparison of activation energies, heats of sorption, and entropic selectivities

Table 7 compares the O_2 and N_2 activation energies for permeation and diffusion as well as heats of sorption for BBL and 6FDA–TADPO. The BBL O_2 and N_2 activation energies for permeation are over 100% greater than the 6FDA–TADPO activation energies. Increases in FFV enable gas molecules to permeate with less resistance, which simultaneously decrease the activation energies for permeation. Considering the 6FDA–TADPO FFV is 70% greater than BBL, the difference in activation energies between the two polymers is not surprising.

Examination of the activation energies for diffusion and heats of sorption, the two factors influencing the activation energy for permeation, provides a more specific structure–property analysis. Again, the activation energy for diffusion primarily influences the permeability changes with temperature since $|E_d| > |H_s|$. For both O_2 and N_2, the BBL activation energy for diffusion is approximately 3.0 kcal/mol greater than that for 6FDA–TADPO. The BBL and 6FDA–TADPO O_2 and N_2 heats of sorption are similar.

Table 9 compares the factors associated with the BBL and 6FDA–TADPO entropic selectivities. Despite the difference in the O_2/N_2 diffusivity selectivities of the two materials, they exhibit a similar *difference* between O_2 and N_2 activation energies for diffusion. $\Delta E_{d,O_2,N_2}$. As BBL possesses a slightly greater $\Delta E_{d,O_2,N_2}$ than 6FDA–TADPO, it exhibits a higher energetic selectivity. Using the diffusivity selectivity and energetic selectivity, the BBL entropic selectivity is calculated to be identical to that of 6FDA–TADPO, a polymer lying on the upper bound trade-off line.

Even though BBL and 6FDA–TADPO exhibit similar entropic selectivities, the performance of 6FDA–TADPO is unquestionably superior. Although the BBL O_2/N_2 permselectivity is higher, the high 6FDA–TADPO permeability pushes its performance to the upper bound trade-off line shown in Fig. 4. Clearly, this is because of higher sorption and diffusion coefficients in 6FDA–TADPO relative to BBL. The higher sorption and faster diffusion results from the more ''open'' polymer matrix. As a result, this study clearly illustrates that increasing entropic selectivity is not the *only* important factor to produce materials near or above the upper bound in Fig. 4. A material with high entropic selectivity will likely exhibit a favorable diffusivity selectivity. Moreover, as the diffusivity selectivity generally controls the permselectivity, such materials will tend to possess a favorable permselectivity. Despite this, a material exhibiting performance on or above the upper bound trade-off line requires *both* a favorable permeability and permselectivity. Using this experimental evidence, a sufficiently ''open'', yet rigid, polymer structure is potentially required to attain an entropically selective high performance polymer.

5. Conclusion

The gas transport and sorption properties of rigid polypyrrolones are greatly influenced by the backbone structure. Producing a highly rigid polymer, which conceivably is able to discriminate between similarly sized penetrants, is not the sole factor in attaining membrane performance that approaches or exceeds the O_2/N_2 upper bound trade-off line. A hyper rigid yet packable polymer such as BBL exhibits extremely low permeabilities coupled with only modest permselectivities. Based on this work, a combination of bulky backbone groups to inhibit chain packing and polymer rigidity is necessary to attain materials with favorable gas separation performance.

Acknowledgements

The authors gratefully acknowledge the support of the Department of Energy's Office of Basic Energy Science under Grant No. DE-FG03-95ER145386, Texas Advanced Research Program, and Medal. In addition, the authors thank Dr. Fred Arnold at Wright Patterson Air Force Base for the dense BBL films used in the permeation experiments.

References

[1] Stern SA. J Membr Sci 1994;94:1.
[2] Koros WJ, Coleman MR, Walker DRB. Annu Rev Mater Sci 1992;22:47.
[3] Cassidy PE. Thermally stable polymers: syntheses and properties. New York: Marcel Dekker, 1980.
[4] Zhou W, Gao X, Lu R. J Appl Polym Sci 1994;51:855.
[5] Zhou W, Lu F. J Appl Polym Sci 1995;58:1561.
[6] Walker DRB. Ph.D.Thesis, The University of Texas at Austin, 1993.
[7] Walker DRB, Koros WJ. J Membr Sci 1991;55:99.
[8] Xuesong G, Zhoushi T, Fengcai L. J Membr Sci 1994;88:37.
[9] Xuesong G, Fengcai L. Polymer 1995;36:1035.
[10] Gao X, Lu F. Gaofenzi Xuebao 1995;4:409.
[11] Gao X, Lu F. J Appl Polym Sci 1996;59:1315.

[12] Jenekhe SA, Tibbetts SJ. J Polym Sci. Polym Phys Ed 1988;26:201.
[13] Hong SY, Kertesz M, Lee YS, Kim O. Macromolecules 1992;25:5424.
[14] Nalwa HS. Polymer 1991;32:802.
[15] Liepins R, Aldissi M. Mol Cryst Liq Cryst 1984;105:151.
[16] Crank J, Park GS. Diffusion in polymers. New York: Academic Press, 1968.
[17] Singh A, Koros WJ. Ind Eng Chem Res 1996;35:1231.
[18] Koros WJ, Fleming GK, Jordan SM, Kim TH, Hoehn HH. Prog Polym Sci 1988;13:339.
[19] Koros WJ. J Polym Sci, Polym Phys Ed 1985;23:1611.
[20] Petropoulos JH. J Polym Sci, Polym Phys Ed 1970;8:1797.
[21] Vieth WR, Howell JM, Hsieh JH. J Membr Sci 1976;1:177.
[22] Koros WJ, Chan AH, Paul DR. J Membr Sci 1977;2:165.
[23] Arnold FE, Deusen RLV. Macromolecular Synthesis 1979;7:31.
[24] Arnold FE, Deusen RLV. Macromolecules 1969;2:497.
[25] Koros WJ, Walker DRB. US Patent 5,262,056, The University of Texas System, 1993.
[26] Costello LM, Walker DRB, Koros WJ. J Membr Sci 1994;90:117.
[27] Breck DW. Zeolite molecular sieves: structure, chemistry and use. New York: Wiley, 1974.
[28] Lide DR, editor. Handbook of chemistry and physics. Boston, MA: CRC, 1990.
[29] O'Brien KC, Koros WJ, Barbari TA. J Membr Sci 1986;29:229.
[30] Costello LM, Koros WJ. Ind Eng Chem Res 1992;31:2708.
[31] Song HH et al. Synthetic Metals 1995;69:533.
[32] Arnold FE, Van Deusen RL. J Appl Polym Sci 1971;15:2035.
[33] Lee WM. Polym Eng Sci 1980;20:65.
[34] Van Krevelen DW. Properties of polymers: their structure and correlation with chemical structure. Amsterdam: Elsevier, 1976.
[35] Bondi AA. Physical properties of molecular crystals, liquids and glasses. New York: Wiley, 1968.
[36] Aitken CL, Koros WJ, Paul DR. Macromolecules 1992;25:3651.
[37] Hellums MW, Koros WJ, Husk GR, Paul DR. J Membr Sci 1989;46:93.
[38] Scott H, Serafin FL, Kronick PL. Polymer Letters 1970;8:563.
[39] Pessan LA, Koros WJ. J Polym Sci, Polym Phys Ed 1993;31:1245.
[40] Robeson LM. J Membr Sci 1991;62:165.
[41] Taylor JR. An introduction to error analysis, 2nd ed. Oxford: University Science, 1997.
[42] Costello LM, Koros WJ. J Polym Sci Polym Phys Ed 1994;32:701.
[43] Costello LM, Koros WJ. J Polym Sci Polym Phys Ed 1995;33:135.
[44] Meares P. J Am Chem Soc 1954;76:3415.
[45] Singh A. Ph.D.Thesis, The University of Texas at Austin, TX, USA, 1997.